

Electrochemical Detection of *BRAF* V600E Mutation in a Liquid Biopsy Format: LAMPing the Way to an Improved Diagnostics and Treatment

Ludmila Moranova, Johana Strmiskova, Katerina Ondraskova, Miroslav Bardelcik, Matous Cwik, Igor Kiss, Roman Hrstka, and Martin Bartosik*

The *BRAF* V600E substitution, predominantly found in melanoma and metastatic colorectal cancer (mCRC), is associated with aggressive traits and poor prognosis. Molecular testing of the *BRAF* mutational status is crucial for guiding therapeutic decisions, driving the necessity for new rapid diagnostic technologies. Here, a novel LAMP-based assay is presented for fast and selective amplification of mutated DNA, coupled with simple electrochemical detection on electrode biochips. The assay demonstrated high selectivity across cell lines and in 51 cancer patients, detecting mutations in both tumor tissue DNA and circulating tumor DNA (ctDNA) in serum. Clear discrimination between the mutated and wild-type sequences is achieved, in perfect agreement with either NGS or ddPCR. The bioassay offers a simple and efficient alternative to traditional PCR methods for point-of-care diagnostics, particularly in settings with limited equipment and resources.

1. Introduction

The *BRAF* proto-oncogene codes a serine/threonine protein kinase, and its mutations lead to ligand-independent activation of the MAPK pathway via phosphorylation of downstream MEK and ERK, ultimately promoting the development and progression of cancer.^[1] The most common alteration in the *BRAF* gene, accounting for ≈90% of cases, is the *BRAF* V600E mutation, resulting from a single nucleotide polymorphism (SNP) at codon 600 (replacement of valine with glutamic acid).^[1b,2] The *BRAF* V600E mutation is observed in ≈10% of mCRC cases, while it is even more prevalent in melanoma, occurring in

up to 50-60% of patients with advanced (unresectable or metastatic) disease.^[2,3] It is associated with an aggressive disease course and is a poor prognostic factor and predictive biomarker in both mCRC and advanced melanoma.^[1b] Agents targeting the mutated *BRAF* oncogene and MEK, such as dabrafenib/trametinib and encorafenib/binimetinib, have shown efficacy and improved outcomes for advanced melanoma patients in several randomized control trials.^[4] Combination therapy is superior to single-agent *BRAF* inhibition and is a standard option for *BRAF*-mutated advanced melanoma.^[5] For *BRAF* V600E mutated mCRC, combined therapy with encorafenib and cetuximab has improved progression-free and overall survival compared to chemotherapy and is the established second-line treatment.^[6] Therefore, molecular testing for the *BRAF* V600E mutation is a key priority in determining the therapeutic approach in both advanced melanoma and mCRC, and it is of great importance that a patient's *BRAF* mutational status is promptly and accurately determined.^[1a,6]

Furthermore, the molecular profile of a tumor can change over time, leading to a 15% discordance in *BRAF* mutational status between primary tumors and metastatic lesions.^[2,7] Therefore, it is recommended to test for *BRAF* mutations in both the primary tumor and recent metastatic lesions.^[2] In addition, the development of acquired resistance to *BRAF* and MEK inhibitors is of significant concern during targeted therapy.^[8] Repeated testing for *BRAF* V600E mutation in blood via liquid biopsy, detecting and monitoring it in cell-free DNA (cfDNA), and analyzing it through molecular biology methods can thus help identify

L. Moranova, J. Strmiskova, K. Ondraskova, R. Hrstka, M. Bartosik
Research Centre for Applied Molecular Oncology
Masaryk Memorial Cancer Institute
Brno 65653, Czech Republic
E-mail: martin.bartosik@mou.cz

J. Strmiskova
National Centre for Biomolecular Research
Faculty of Science
Masaryk University
Brno 62500, Czech Republic

M. Bardelcik
Department of Oncological Pathology
Masaryk Memorial Cancer Institute
Brno 65653, Czech Republic

M. Bardelcik
Department of Biochemistry
Faculty of Science
Masaryk University
Brno 62500, Czech Republic

M. Cwik, I. Kiss
Department of Comprehensive Cancer Care and Faculty of Medicine
Masaryk Memorial Cancer Institute and Masaryk University
Brno, Czech Republic

 The ORCID identification number(s) for the author(s) of this article can be found under <https://doi.org/10.1002/admt.202401404>

© 2024 The Author(s). Advanced Materials Technologies published by Wiley-VCH GmbH. This is an open access article under the terms of the [Creative Commons Attribution](https://creativecommons.org/licenses/by/4.0/) License, which permits use, distribution and reproduction in any medium, provided the original work is properly cited.

DOI: 10.1002/admt.202401404

patients with acquired resistance and monitor treatment response in *BRAF*-mutated advanced melanoma and CRC.^[2,7,9]

Next-generation sequencing (NGS) is currently the method of choice that offers high-throughput screening of a large panel of point mutations across the genome, yet it remains costly, laborious, and data-intensive for eventual application in low-resource settings or at the point-of-care (PoC). PCR-based techniques, including real-time PCR or digital PCR, are faster and less expensive than NGS but also require relatively large instrumentation and skilled personnel. Thus, there is a need for simple, fast, and cost-effective technologies for *BRAF* V600E mutation detection to monitor treatment response. In this context, isothermal amplification techniques (IATs) offer rapid amplification at steady moderate temperatures without the need for thermal cycling and show higher resistance to PCR inhibitors.^[10] Loop-mediated amplification (LAMP) is perhaps the most well-known IAT, with similar or even higher sensitivities than PCR, using *Bst* polymerase and four to six primers to rapidly amplify nucleic acids at elevated temperatures between 55 and 70 °C. Previously, we reported several IAT-based bioassays coupled to an electrochemical (EC) end-point detection system with inexpensive compact instrumentation and the option of fast parallel measurements at electrode chips,^[11] including LAMP-based assays where we determined HPV infection in precancerous cervical lesions^[11a-c,e] or RNA biomarkers in the urine of prostate cancer patients.^[11d] The application of LAMP for SNP analysis is less common because the design of SNP-specific LAMP primers is quite challenging. Hence, SNP-specific DNA probes are the most commonly used. Only a few studies have demonstrated SNP-specific LAMP primers targeting, e.g., *MTHFR* or *ALDH2* genes, but none of them utilized EC detection.^[12]

Here, we describe for the first time a simple, rapid, and straightforward LAMP-based assay combined with EC detection for the analysis of the *BRAF* V600E mutation. The assay demonstrated excellent performance in melanoma and CRC patient samples, for both DNA from tumor tissues and circulating tumor DNA (ctDNA) in serum. A clear discrimination of the *BRAF* V600E mutation from the wild-type (wt) sequence was obtained, which perfectly correlated with NGS or droplet digital PCR (ddPCR) data. Thus, our bioassay could be particularly useful for PoC diagnostics where equipment and resource limitations may pose challenges for traditional PCR methods.

2. Results and Discussion

2.1. Assay Principles

The overall assay is straightforward and involves only a few simple and time-effective steps. Extracted DNA was used as a template for the LAMP reaction with SNP-specific primers, which recognized only the V600E variant of the *BRAF* gene (Figure 1A, 30 min) but not the wt variant. During the LAMP reaction, *Bst* polymerase randomly incorporated biotinylated dUTPs alongside classical dTTPs, generating a biotinylated product. This was followed by hybridization of biotinylated LAMP products with mutation-specific locked nucleic acid (LNA) probes attached to carboxylic magnetic beads (MBs) (Figure 1B, step 1, 15 min) and incubation with streptavidin peroxidase polymer (SPP) that interacted with biotin moieties incorporated within the LAMP prod-

uct (Figure 1B, step 2, 15 min). We utilized a polymeric form, the SPP, where the streptavidin protein is covalently linked to a polymerized version of the horseradish peroxidase enzyme. Finally, electrochemical readout of the peroxidase reaction (Figure 1B, step 3, 1 min) was performed on an 8-electrode carbon array that enabled the simultaneous analysis of eight samples to speed up the entire measurement (Figure S1, Supporting Information).

The assay was thoroughly optimized at multiple levels, as detailed in the Supplementary Information (Table S1, Supporting Information). Various conditions were tested to decrease the overall assay time while maintaining a high signal-to-noise ratio. For the LAMP reaction, two sets of primers were used, each for a different gene. The first primer set targeted *BRAF* and was designed to distinguish only the V600E mutated variant (mut DNA). This was achieved by positioning the 5'-end of both FIP and BIP primers at the mutated site. Loop primers were introduced to shorten an overall LAMP reaction time from 60 to 30 min (Figure S2, Supporting Information). The second set of LAMP primers was designed for the *ACTB* gene (beta-actin), which served as a positive control for the quantity and integrity of the DNA sample, preventing false-negative results. To ensure the same duration of the LAMP reaction, loop primers for *ACTB* were also introduced, yielding strong band intensities across all cell lines (Figure S3, Supporting Information). The final LAMP setup involved a 30-min reaction time at a temperature of 62 °C for both genes.

The final LAMP mixture, in addition to the four classical dNTPs, also contained biotin-labeled dUTP nucleotides that could be enzymatically incorporated into the LAMP product (as we have shown previously,^[11b,d] to bind with the SPP for facilitated end-point detection. To improve the specificity of the V600E determination, LNA capture probes attached to MBs were employed due to their ability to discriminate single mismatch variations.^[13] The 15-nt LNA probes consisted of 12 deoxyribonucleotides and 3 consecutively inserted LNA nucleotides (forming a triplet) positioned centrally within the probe around the mutation site. The point mutation was located in the middle of this triplet (refer to Table S2, Supporting Information). To prevent the formation of DNA secondary structures of the LAMP products, a denaturation step (95 °C for 10 min, followed by ice cooling) was first performed. The final assay time, including the LAMP reaction, incubation, and measurement time, was ≈70 min without hands-on time and < 2 h including hands-on time (based on the number of samples per run).

2.2. Analytical Characteristics

Specific primer design is crucial for accurate SNP analysis. This was ensured by positioning the 5'-ends of both FIP and BIP primers at the mutated site. To check the selectivity of the LAMP primers toward the V600E mutation, all designed sets were tested using DNA extracted from a panel of cancer cell lines with different mutation status (Figure 2A,B). This panel included the A375 cell line with V600E mutation in both alleles (V600E/V600E), HT29 as a V600E heterozygote (V600E/wt), and Caco2, SW620, LAPC4, and PANC1 cancer cell lines with only the wt sequence (wt/wt).

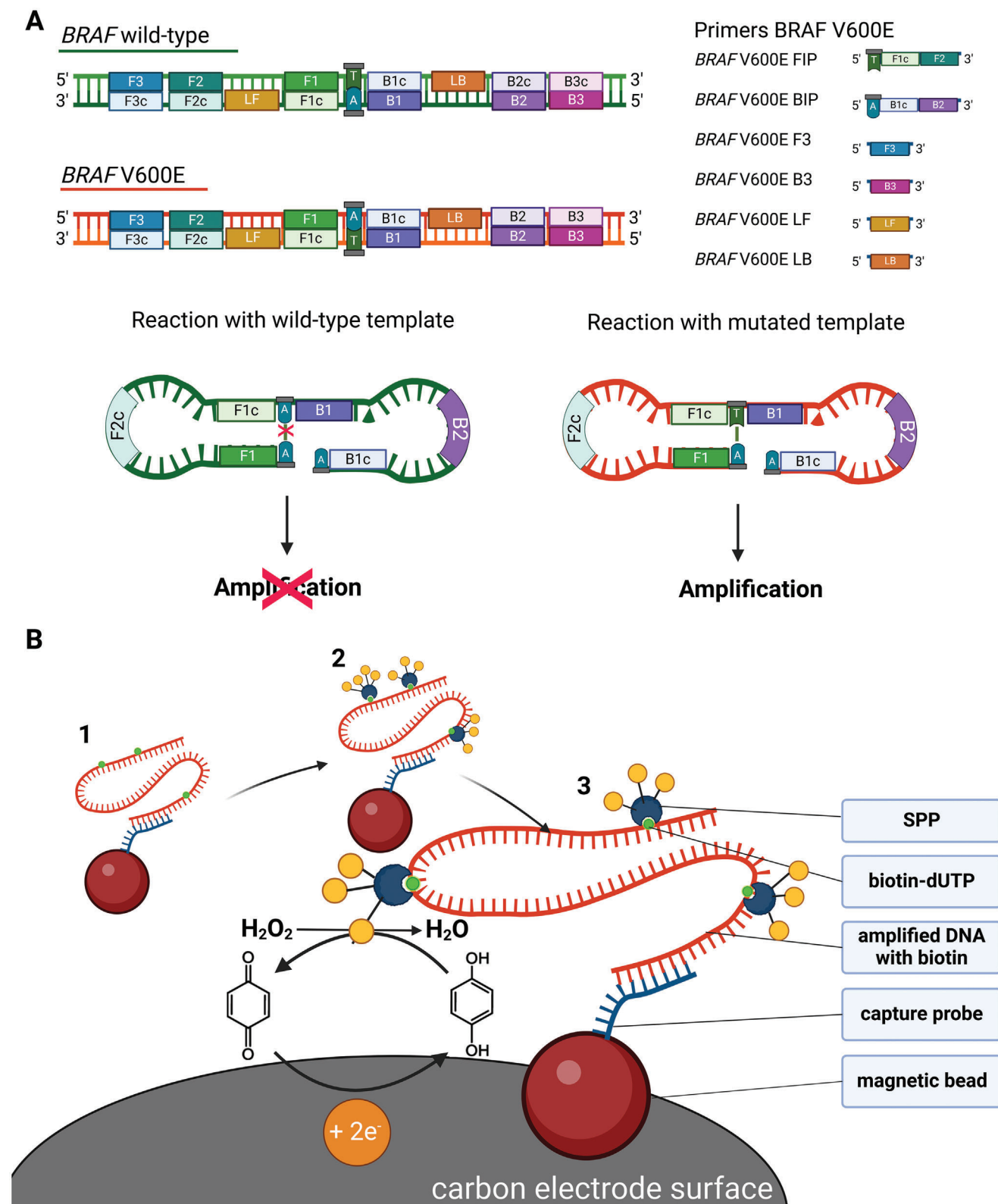


Figure 1. Scheme of the bioassay. A: Principle of SNP-specific primers for *BRAF* V600E detection showing their positions within DNA templates. The overlapping 5' ends of the FIP and BIP primers are crucial for specific recognition. The reaction proceeds only in the presence of V600E mutation (right), but not in the wt variant (left). B: 1) Amplified LAMP products with incorporated biotin-dUTP hybridize with LNA capture probes on magnetic beads, 2) followed by SPP labeling which binds to biotin moieties within the LAMP product, and 3) amperometric measurement of the SPP-catalyzed reaction involving the hydroquinone and hydrogen peroxide couple and a carbon electrode chip consisting of 8 working electrodes.

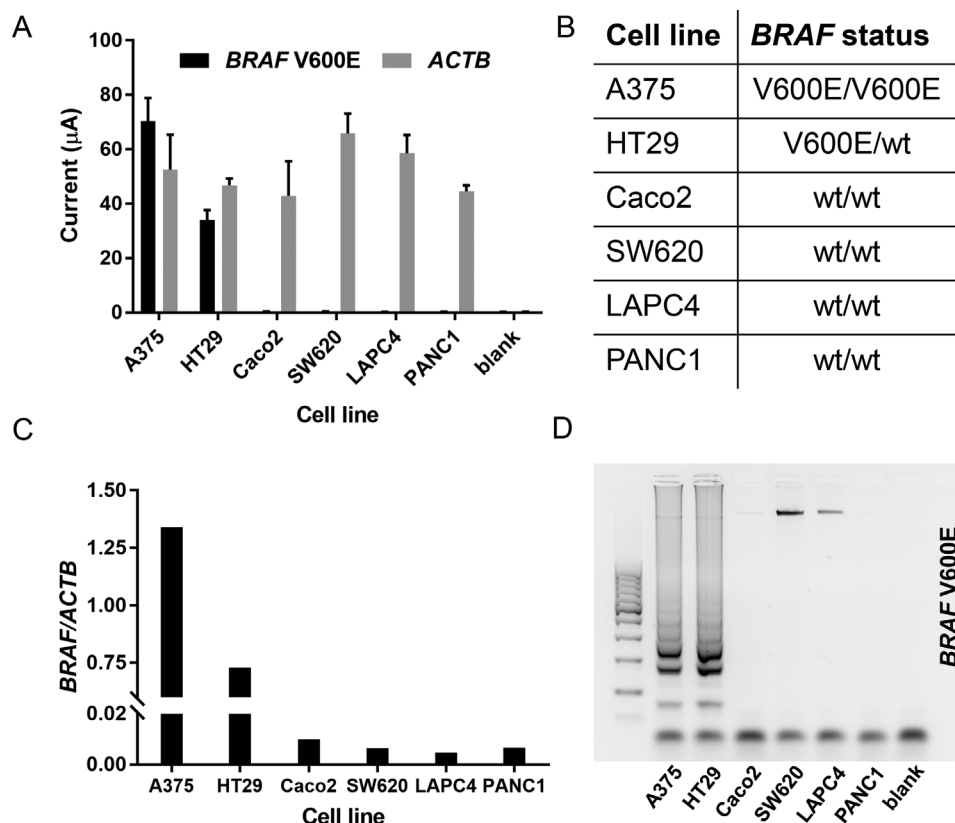


Figure 2. Selectivity assay. A: Electrochemical analysis of DNA from cancer cell lines using *BRAF* V600E and *ACTB* primers for LAMP reaction. B: *BRAF* V600E mutation status of used cell lines. C: Ratio of EC values between *BRAF* V600E and *ACTB* from graph in 2A. D: Visualization of LAMP products on agarose gel using *BRAF* V600E primer set.

The SNP-specific primers (*BRAF* V600E in Table S2, Supporting Information) correctly recognized mutated sequences in all the tested cell lines (Figure 2A, black bars). The highest signal was obtained for A375 DNA (V600E/V600E), followed by HT29 DNA, where the EC current decreased by $\approx 50\%$. The rest of the cell lines (wt/wt) showed signals at levels close to those of the blank sample (i.e., non-template control, NTC). Moreover, a second set of primers targeting the *ACTB* gene as an internal control was used on the same panel of cell lines (Figure 2A, grey bars). The *ACTB* primers amplified DNA in all cells, confirming that the template DNA was of sufficient quality, and no signal was obtained from the blank. EC signals for *ACTB* primers slightly varied among each other (within the range of SD), possibly due to different DNA content. Hence, a ratio of *BRAF*/*ACTB* currents was calculated to normalize *BRAF* signals to the internal control across all cell lines (Figure 2C). It will be shown below that this ratio can be particularly useful for clinical sample analysis, where a large variability of the sample quality and quantity is expected. To validate the EC data, gel electrophoresis after the LAMP reaction was carried out, showing successful amplification of A375 and HT-29 samples, whereas no amplification occurred for other cell lines (Figure 2D). To prevent false positives by accidentally exchanging LAMP products, a cross-reactivity experiment was carried out that showed very good selectivity of CPs toward their matching LAMP products (Figure S4, Supporting Information).

The analytical sensitivity of the assay was tested for both genes using two different sample sets (Figure 3). The first set comprised DNA isolated from the A375 cell line carrying only the V600E mutation (V600E/V600E). The second set contained a mixture of mut DNA (20%) from A375 cancer cells and wt DNA (80%) from SW620 cancer cells. This set was chosen because of the large heterogeneity of clinical specimens, which often comprise both tumor and non-tumor cells. The ratio (20% mut/80% wt) was intentionally chosen based on the content of mutated DNA in clinical samples determined by NGS (where the median of the V600E mutation was 37%, Table S3, Supporting Information). By testing these two samples (100% and 20% mut DNA) with different dilutions (final concentration of DNA in LAMP reaction was between 0.01 and 20 ng μL^{-1}), it was possible to distinguish *BRAF* V600E mutation already in 0.1 ng μL^{-1} of 100% mutated sample and in 0.5 ng μL^{-1} of 20% mut (Figure 3A,B). When using *ACTB* primers, as little as 0.1 ng μL^{-1} of both samples could be determined (Figure 3C,D) because the *ACTB* amount was the same regardless of the mutation status. Due to relatively large standard deviations at low sample concentrations, it is recommended to use at least 5 ng per sample (0.5 ng μL^{-1}). Furthermore, an experiment where an increasing amount of mutated DNA (from 0.1 to 5 ng) was spiked into an excess constant amount of wt DNA (100 ng) was performed. The results are shown in Figure S5 (Supporting Information), indicating that as little as 0.05 ng μL^{-1} (or 0.5 ng) of mutated DNA can be determined. In other words,

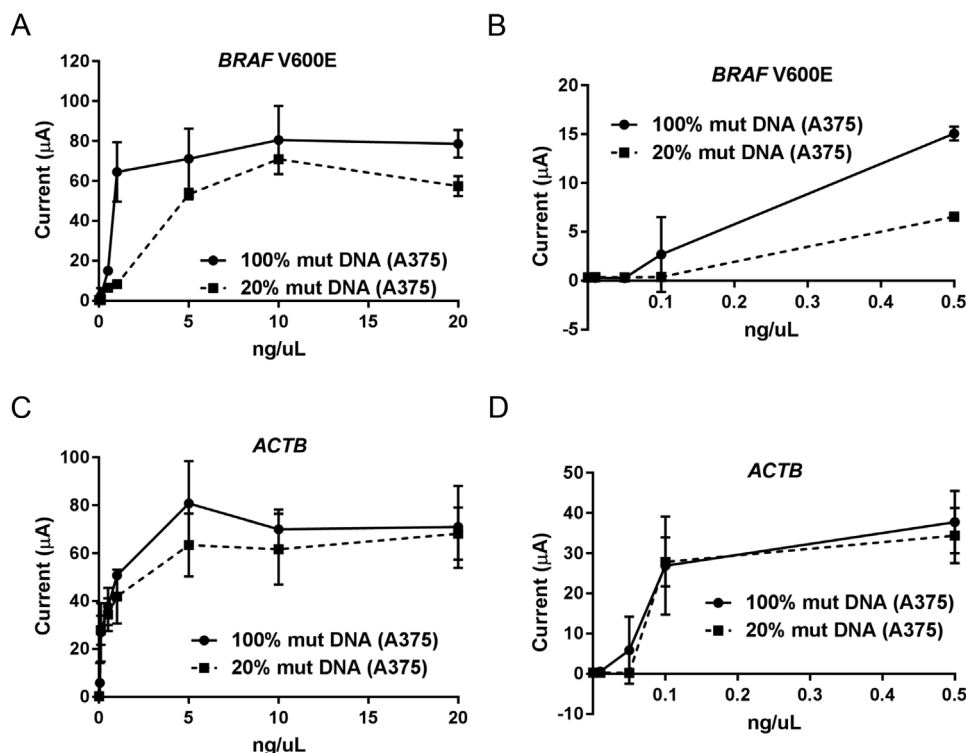


Figure 3. Analytical sensitivity. 100% mut DNA was extracted from A375 cell line, which harbors V600E mutation in both alleles; 20% mut DNA represents a mix of 20% mutated DNA (A375) and 80% wt DNA (SW620). A: EC measurements of *BRAF* V600E. B: Detail of the lower concentrations from 3A. C: EC measurements of *ACTB* gene. D: Detail of the lower concentrations from 3C.

V600E mutated DNA can be detected when it constitutes only 0.5% of the sample DNA, the rest being wild type.

A stability experiment was also performed to evaluate the performance of the CP-modified MBs over a longer period (modified magnetic beads were stored in PBS with 0.02% sodium azide at 4 °C), showing good stability for at least two months (RSD for positive samples were 12.60% and 6.99%, Figure S6, Supporting Information). The high analytical sensitivity of our bioassay is largely due to the LAMP reaction. However, other factors may have contributed to the increased sensitivity, such as the use of an ultrasensitive SPP as a polymeric variant of streptavidin-peroxidase conjugates, or pre-concentration of MBs at the surface of the electrode. For instance, the signal increased with a higher amount of MBs (due to the presence of a higher number of SPP), but decreased again when the electrode surface became oversaturated with an excessive amount of MBs, inhibiting the resulting electron flow from the electrode to the oxidized substrate (Figure S7, Supporting Information). This was also the reason why we normalized the amount of MBs after the modification step with LNA by measuring the optical density (OD600) of individual batches. This finding is further supported by an experiment comparing normalized and non-normalized (i.e., constant) volumes used for the analysis of V600E *BRAF* DNA sequence (Figure S8, Supporting Information). For this, we have used three different batches by changing the amount of MBs entering the modification reaction (the original amount referred to as 100%, the amount decreased by 25%, and the amount increased by 25%). Without a normalization, i.e., when using a con-

stant volume of MB regardless of the batch used, current values show higher fluctuation (black bars) than after the normalization, i.e., by adjusting MB volume based on the optical density measurement (grey bars).

2.3. Patient Samples

The bioassay was applied to clinical specimens to demonstrate its feasibility. First, 31 DNA samples from tumor tissue were examined. NGS data showed that 13 of them harbored no mutation (*wild-type*, samples wt1-13), while the remaining specimens (mut1-18) displayed V600E mutation frequencies ranging from 11% to 81% relative to the DNA content (more details in Table 1; Table S3, Supporting Information). Our data confirmed these findings, as shown in Figure 4 and Figure S9 (Supporting Information). However, four tissue samples out of 31 were negative for *ACTB* (EC values under 1 μA, Table S4, Supporting Information), reflecting the lower quality of the samples, and thus they do not appear in the graphs. The remaining samples perfectly correlated with the NGS data (Figure 4A,B), correctly identifying all 15 mutated and 12 wild-type samples with high significance ($p < 0.001$).

The dots in Figure 4 represent the mean values of duplicate measurements. The calculated ratios of these mean values (*BRAF*/*ACTB*) are shown in Figure 4C ($p < 0.001$). This ratio helps normalize *BRAF* signals based on the quality and amount of the present DNA (because a wide range of EC signals was

Table 1. Clinicopathological characteristics of patient samples.

	Samples	N	Age, Median	Sex: F/M	Type of tumor: CRC/Mel	TNM	Grade [CRC] ^{a)}	Neoadjuvant therapy [CRC] ^{b)}	Other malignancy
Tissue N = 31	Wild-type (wt)	13	44-80, 66	4/9	11/2	II (3)	G1 (3)	YES (1)	YES (3)
						III (7)	G2 (6)	NO (9)	NO (6)
						IV (3)	G3 (1)	UNK (1)	UNK (4)
							UNK (1)		
	V600E (mut)	18	49-86, 70	11/7	12/6	II (4)	G1 (1)	YES (0)	YES (5)
						III (10)	G2 (5)	NO (12)	NO (10)
						IV (4)	G3 (6)		UNK (3)
Serum N = 27	Wild-type (wt)	12	59-83, 69	5/7	2/10	I (2)	G1 (1)	YES (0)	YES (8)
						II (5)	G2 (1)	NO (2)	NO (4)
						III (5)			UNK (0)
	V600E (mut)	15	30-80, 59	9/6	5/10	II (1)	G2 (2)	YES (0)	YES (2)
						III (12)	G3 (3)	NO (5)	NO (13)
						IV (2)			UNK (0)
All patients ^{c)} N = 51	Wild-type (wt)	23	44-83, 70	9/14	11/12	I (2)	G1 (3)	YES (1)	YES (10)
						II (8)	G2 (6)	NO (10)	NO (9)
						III (10)	G3 (1)		UNK (4)
						IV (3)	UNK (1)		
	V600E (mut)	28	30-86, 66	16/12	12/16	II (5)	G1 (1)	YES (0)	YES (5)
						III (18)	G2 (5)	NO (12)	NO (20)
						IV (5)	G3 (6)		UNK (3)

^{a)} In malignant melanoma, the grading is not established; ^{b)} Neoadjuvant therapy was not the standard of care at the time of data collection and has not been established to date; ^{c)} Seven patients are included in both tissue and serum cohorts, i.e., total of 58 clinical specimens were obtained from total of 51 patients; UNK – unknown; CRC – colorectal carcinoma; Mel – melanoma.

obtained when determining *ACTB*). The table in Figure 4D provides more details on the EC data, along with the test accuracy as compared to NGS.

Afterward, the bioassay was tested on 27 serum samples to check for the *BRAF* V600E mutation in ctDNA. The *BRAF* mutation status of patients has been analyzed using NGS or Cobas methodology, although the analysis itself was not conducted on serum samples, but rather on DNA extracted from corresponding tissue samples. This approach ensures a more accurate representation of the molecular profile of the tumor, providing valuable insights into the genetic alterations present in the tumor. NGS/Cobas revealed 15 *BRAF* V600E samples and 12 wt samples. All serum samples were subjected to the same procedure as that used for the tissue cohort to assess *BRAF* V600E (Figure 5A), *ACTB* (Figure 5B), and *BRAF/ACTB* ratio (Figure 5C). Analogous to the tissue cohort, one sample (wt25) exhibited insufficient DNA quantity based on the *ACTB* signals (Table S4, Supporting Information) and was thus eliminated from the data analysis. Our EC data were compared with ddPCR analysis conducted on identical ctDNA samples isolated from the serum (Figure S9, Supporting Information). By comparing these two methodologies, we achieved a sensitivity and specificity of 100% (Figure 5D). Furthermore, ddPCR yielded a negative result for sample wt25, further confirming our data interpretation.

It is worth mentioning that paired tissue and serum samples were only obtainable from seven patients (EC results in Figure S10, Supporting Information), with the remaining patients providing either tissue or blood samples, but not both. To mitigate potential discrepancies arising from differences between tissue and serum as sample sources, our EC data from tissue samples were compared with the NGS/Cobas methodol-

ogy (performed with the same tissue samples), and EC data from serum samples were compared with ddPCR (performed with the same serum samples). With this approach, a perfect accuracy of our test was obtained, reaching 100% sensitivity, specificity, and predictive values when compared to standard techniques. Similarly, the receiver operating characteristic curves shown in Figure S11 (Supporting Information) revealed perfect diagnostic accuracy. The areas under the curve reached values of 1 in all cases, i.e., for tissue samples (when compared to NGS, the optimal threshold is 5.237 μ A) and serum samples (compared with ddPCR, the optimal threshold is 1.632 μ A), both with or without normalization to beta-actin signals. Of course, with a larger cohort of patients, these numbers will most likely decrease. Additionally, when comparing our EC data obtained from serum with NGS/Cobas from tissue, the overall agreement decreased, reaching a sensitivity of 93% and specificity of 83% (Table S5, Supporting Information). This is not surprising because in recent tumor mutational burden (TMB) studies, it has been proposed that blood TMB cannot be substituted for tissue TMB, but rather serves as an index that encompasses tumor heterogeneity and provides different predictive values than tissue TMB.^[14]

3. Conclusion

Our results indicate that this simple and rapid bioassay can detect the *BRAF* V600E mutation with high selectivity and sensitivity. Table S6 (Supporting Information) compares the overall time of the NGS (>1 day) and ddPCR workflow (>6 h) with our bioassay (<3 h). Recently, novel biosensing approaches for V600E analysis have emerged, involving, e.g., amperometric,^[15] colorimetric,^[16] fluorescence^[17] or surface-enhanced Raman spectroscopy^[18]

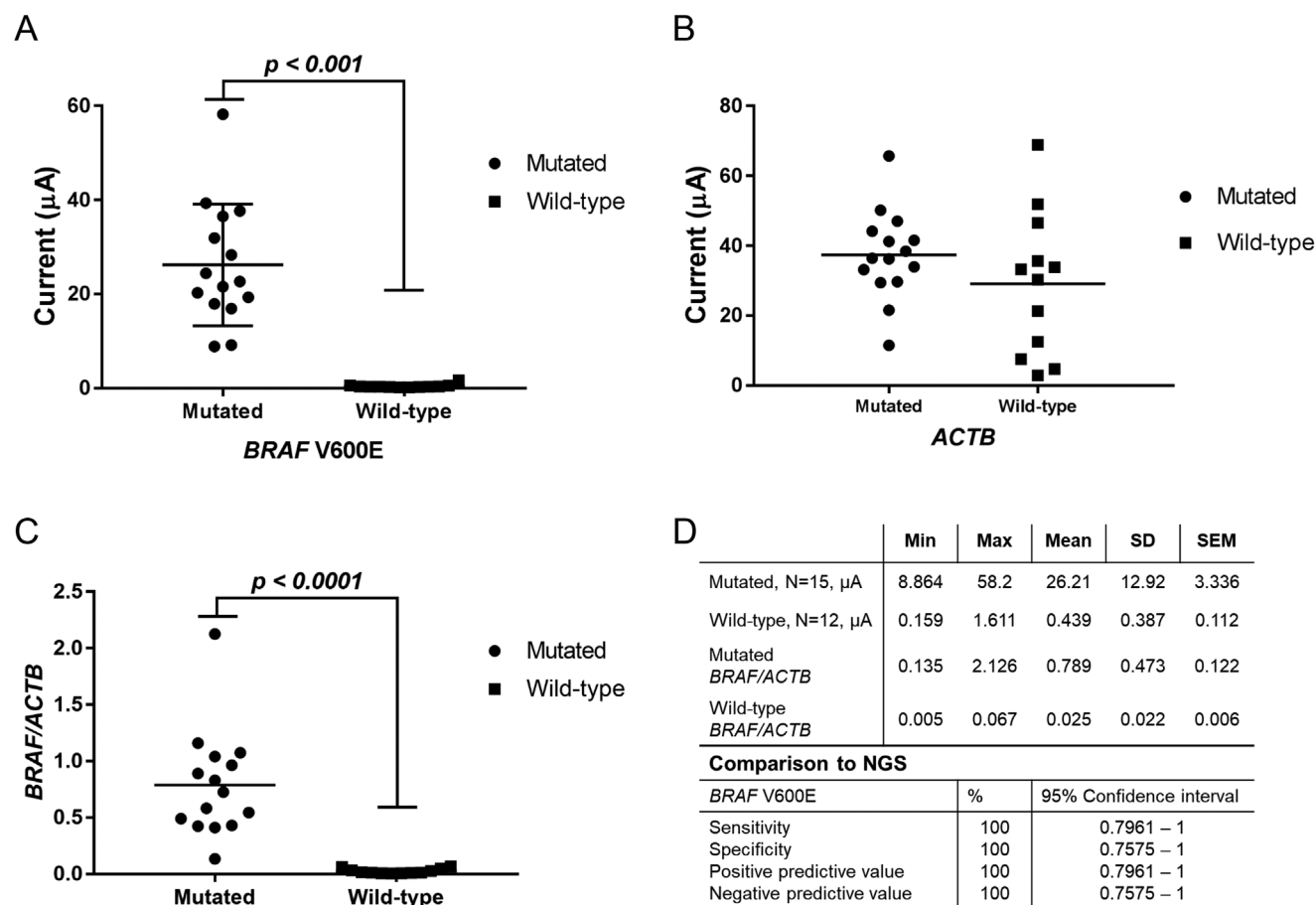


Figure 4. EC data from the tissue samples. A: Dot plot of tissue samples amplified using *BRAF V600E* primers. The samples were divided into two groups (mutated, wild-type) based on NGS data. Each dot represents the mean value from duplicate measurements. The difference between the two groups was highly significant ($p < 0.001$). B: Analogous dot plot using the *ACTB* primers. C: Dot plot of the *BRAF/ACTB* ratio. Horizontal lines represent the mean values of the two groups (mutated, wild-type). D: Statistical data from the EC measurements. Sensitivity and specificity were calculated using the chi-squared test and compared with NGS.

readout systems. Although these strategies demonstrated excellent sensitivities, they mostly utilized PCR and were not directly applied to the patient's blood for analysis of ctDNA. Importantly, some interesting strategies have appeared that utilized also LAMP reaction coupled with various end-point detections, e.g. optical detection using dip strips,^[19] fluorescence readout^[20] or colorimetric visualization,^[21] but again, they mostly used synthetic targets or their spiking into the human plasma. A colorimetric strategy by Papadakis et al. has been demonstrated on twelve FFPE samples, which is an important step toward clinical diagnostics.^[21] To our knowledge, we report here for the first time a LAMP-based strategy for ctDNA analysis in the blood serum of cancer patients without any spiking, along with a positive *ACTB* control to check the quality of the sample. Moreover, our LAMP primers are extremely selective and amplify only V600E sequence, not a wild-type. Hence, there was no need to use any blocker or clamping probe to suppress wt amplification, or any detection probe in subsequent steps. At the cell line level, the LAMP primers demonstrated exceptional selectivity toward the mutation, as confirmed by both EC data (Figure 2A) and gel electrophoresis (Figure 2D), where virtually no amplification

proceeded with the wt sample. This is due to a specific design of overlapping FIB and BIP primers, where nucleotides at the V600E mutation site in both template DNA strands were bound to the FIP and BIP LAMP primers, respectively. Indeed, when using one-base shorter BIP primer that did not overlap the mutated site (*BRAF UNI_BIP*, Table S2, Supporting Information), amplification of the V600E/V600E variant (A375) was slightly less effective (Figure S12, Supporting Information). Moreover, a faint non-specific amplification pattern was observed for the wt/wt variant (SW620). None of these appeared when overlapping primers (*BRAF V600E_FIP* and *BRAF V600E_BIP*) were used. When clinical samples were involved, the wt samples exhibited weak smears in the gel (Figure S13, Supporting Information), which could possibly be evaluated as false-positive results. In our EC-based approach, the LNA capture probes conferred extra specificity to resolve these ambiguous gel results, providing only negligible signals from wt samples at the level of a blank measurement (Figures 4A and 5A; Figure S9, Supporting Information).

Our data also emphasize the importance of internal quality control, provided by measuring *ACTB* presence. Although

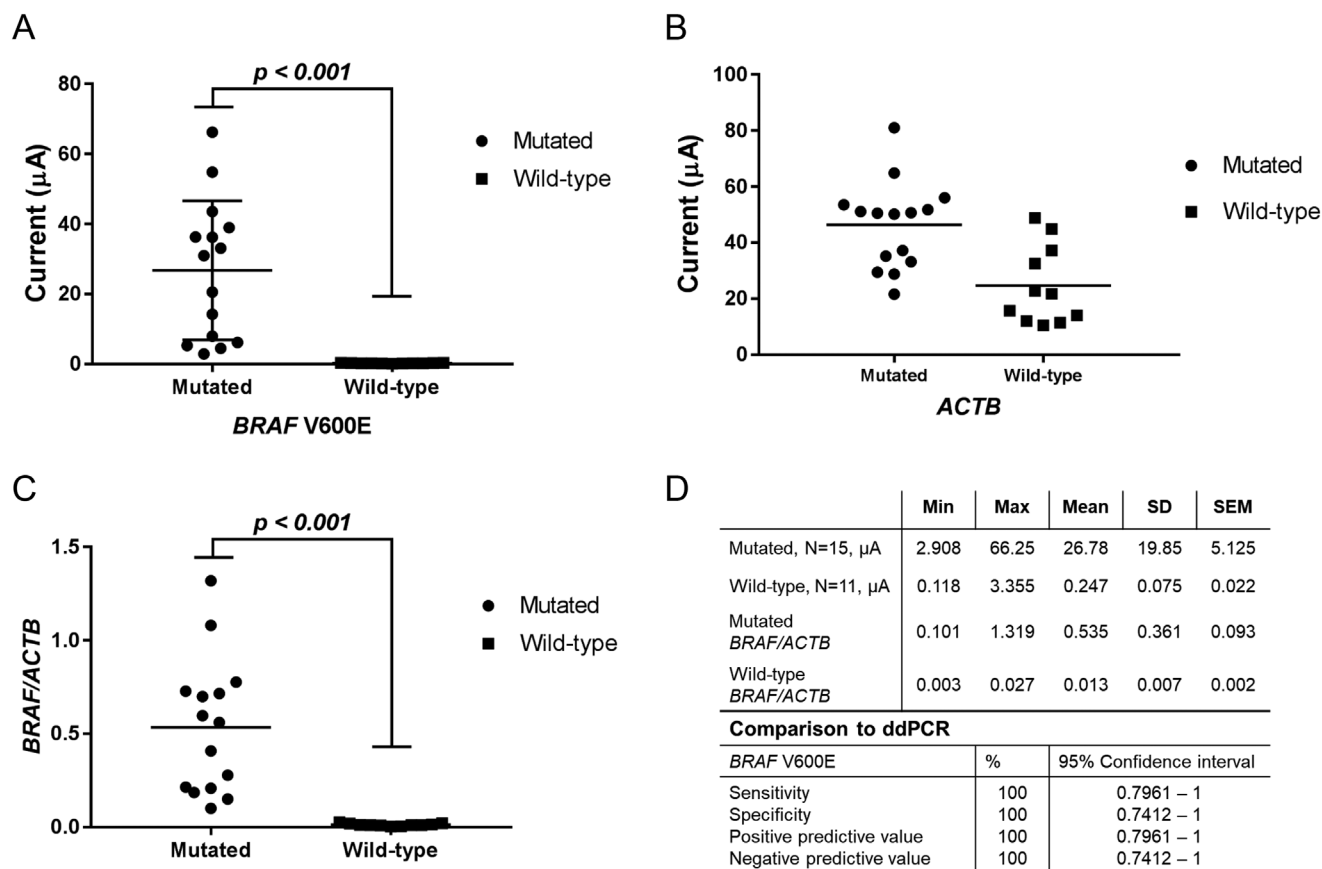


Figure 5. EC data from the serum samples. A: Dot plot of serum samples amplified using *BRAF V600E* primers. The samples were divided into two groups (mutated, wild-type) based on NGS data. Each dot represents the mean value from duplicate measurements. The difference between these two groups was highly significant ($p < 0.001$). B: Analogous dot plot using the *ACTB* primers. C: Dot plot of the *BRAF/ACTB* ratio. Horizontal lines represent the mean values of the two groups (mutated, wild-type). D: Statistical data from the EC measurements. Sensitivity and specificity were calculated using the chi-squared test and compared with ddPCR.

routinely used in standard techniques, such as real-time PCR, this is not often exploited in biosensor studies. Indeed, three of our tissue samples and one serum sample yielded low *ACTB* signals, reflecting their low quality (as confirmed by ddPCR). Without this quality control, the samples were evaluated as having wild-type DNA. Based on our experience, we recommend repeating measurements with *ACTB* signals under $10 \mu\text{A}$ and, if possible, increasing DNA input into the reaction (for both biomarkers) to ensure the validity of the results.

To conclude, reliable detection of DNA point mutations is crucial in contemporary oncological research, driving the development of new techniques with improved selectivity and sensitivity. Moreover, noninvasive liquid biopsy testing of ctDNA is of paramount importance for early detection of cancer or monitoring of patient treatment, and new methods should integrate this crucial aspect to improve their clinical efficacy. The LAMP is a fast and ultrasensitive alternative to PCR that amplifies DNA at a constant temperature, eliminating the need for a thermal cycler. When coupled with electrochemical readout offering cost-effective, simple, and miniaturized instrumentation with the option of parallel measurements on electrode chips. Indeed, when comparing our assay with ddPCR or NGS, the estimated cost of chemicals and materials in our assay per one sample is ≈ 3 EUR,

or ≈ 37 EUR for complex analysis of a single patient including triplicate measurements of a test sample and a non-template control for both *BRAF* and *ACTB* primers. The same complex analysis per single patient is roughly 115 EUR for ddPCR, 85 EUR for digital PCR in a non-droplet mode, and ≈ 140 EUR using TruSight Oncology 500 panel in NGS. This highlights a great cost reduction in chemicals and materials when using our assay. Moreover, small portable potentiostats are very affordable. Our technology could thus prove useful for ctDNA detection in PoC settings outside large laboratories, ideal for decentralized medicine. To facilitate the transition toward PoC, it would be beneficial to exclude the DNA extraction step. As a matter of fact, we have shown previously that the LAMP performs well also in cell or tissue lysates without a need for a preceding DNA extraction step.^[11c] For blood samples, it is expected that some pretreatment would be needed to remove inhibitors for LAMP (as well as PCR or other amplification techniques) to function well.

4. Experimental Section

Materials: Master mix for LAMP reaction (Saphir Bst Turbo Green-Master) and biotin-16-dUTP were from Jena Bioscience (Germany), Sera-Mag Carboxylate-Modified Magnetic Beads (MB) were from

Cytiva (USA), and casein blocking buffer (CBB, sold as Blocker Casein) were from Thermo Fisher Scientific, 2-(N-morpholino)ethanesulfonic acid (MES), potassium chloride, EDTA, streptavidin-peroxidase polymer (SPP) and hydroquinone were from Merck, boric acid, sodium chloride, sodium phosphate dibasic dodecahydrate and potassium phosphate monobasic were from Lachner (Czech Republic), sodium phosphate monobasic dehydrate was from Penta (Czech Republic), Tris-HCl was from Affymetrix (USA), agarose for gel electrophoresis, 1-ethyl-3-(3-dimethylaminopropyl)carbodiimide (EDC) and Tris base were from The Carl Roth GmbH (Germany) and GelRed nucleic acid gel stain was from Biotium (USA). All other chemicals were of analytical grade, and all solutions were prepared in deionized water. DNA LAMP primers/probes were designed using PrimerExplorer V.5 software (<https://primerexplorer.jp>) and synthesized by Generi Biotech (Czech Republic). LNA-containing capture probes (Affinity Plus single-stranded DNA) were synthesized by Integrated DNA Technologies (USA). The sequences of all the oligonucleotides are listed in Table S2 (Supporting Information). Modified magnetic beads were quantified using Eppendorf 6131 Biophotometer Spectrometer (Germany). Electrochemical measurements were performed on multipotentiostat/galvanostat μ Stat 8000 (Metrohm DropSens, Spain) connected to an electrochemical array of eight cells, each in a three-electrode setup (Metrohm DropSens, DRP-8 \times 110) controlled by DropView software. A horizontal gel electrophoresis system (Sub Cell GT Cell and Mini-Sub Cell GT Cell) was obtained from Bio-Rad (USA). Following buffers were used: MES buffer for magnetic beads modification (25 mM MES buffer, pH 5.0); TBE buffer for gel electrophoresis (0.1 M Tris base, 0.1 M boric acid and 2 mM EDTA, pH 8); washing buffer (WB) for magnetic beads (1 M NaCl, 0.5 mM EDTA and 5 mM Tris-HCl, pH 8.5); phosphate buffer (PB, 0.1 M sodium phosphate buffer, pH 6.0); 1 \times PBS (0.14 M NaCl, 2.7 mM KCl, 1.5 mM KH_2PO_4 , 6.4 mM Na_2HPO_4).

Cell Lines and Clinical Samples: The A375, HT-29, Caco2, SW620, LAPC4, PANC1, and HeLa cell lines were cultivated in Dulbecco's Modified Eagle's Medium (DMEM) containing 10% fetal bovine serum, 1% penicillin-streptomycin, and 1% pyruvate. All the cell lines were cultivated at 37 °C, 100% air humidity, and 5% CO_2 . The cellular suspension was centrifuged (1500 rpm, 5 min), supernatant was discarded and pellets were stored at –80 °C. DNA from the cell lines was extracted using the Tissue DNA Preparation Column Kit (Jena Bioscience, Germany) according to the manufacturer's instructions.

The study was approved by the Ethical Committee of Masaryk Memorial Cancer Institute (2020/1496/MOU), and informed consent was obtained from all patients enrolled in the study. Patient samples were collected in a time period 2014–2021 at Masaryk Memorial Cancer Institute. Serum samples were collected prior to surgery, while the tissues were obtained during surgery. DNA extraction from formalin-fixed paraffin-embedded tissues was performed using the QIAamp DNA FFPE Tissue Kit (Qiagen, Germany), following the manufacturer's instructions. DNA concentration was measured on a Qubit Fluorometer 3.0, with a Qubit dsDNA HS Assay Kit (Thermo Fisher Scientific, USA). Sequencing of 40 clinical samples was performed on a MiSeq instrument (Illumina, USA), and the mutation status was evaluated using the NextGENe software (SoftGenetics, USA). The minimum allele frequency was set to 5%, and the minimum coverage of sequenced regions (300 \times) was checked using IGV (Broad Institute) and/or NextGENe. The remaining samples (N = 11) were evaluated using Cobas technology for BRAF V600E mutation status.

Blood samples from CRC and melanoma patients (Table 1) were collected into EDTA tubes and centrifuged within 30 min to extract the serum. The extracted serum was immediately stored at –20 °C and transferred to –80 °C within two weeks. The samples were then stored in the Bank of Biological Material at the Masaryk Memorial Cancer Institute (BBM MMCI) at –80 °C. A Plasma/Serum Cell-Free Circulating DNA Purification Mini Kit (Norgen Biotek Corp.) was used to isolate cfDNA from the serum. Frozen samples were centrifuged at 400 \times g for 2 min at 4 °C. Then, 500 μ L of serum was pipetted into a 2 mL tube. After adding 30 μ L Proteinase K, the mixture was vortexed for 10 s and incubated at 60 °C for 10 min. Isolation was performed according to the manufacturer's protocol. The volume of the eluted DNA was 35 μ L. A Qubit dsDNA HS Assay Kit (Invitrogen) was

used to determine the amount of cfDNA obtained. The concentration of the isolated cfDNA varied from 0.095 to 5.83 ng μL^{-1} . For LAMP reaction and ddPCR, 3.45 and 5 μ L per reaction were used, respectively.

LAMP Reaction: Final LAMP reaction mixture contained 1 \times Saphir Bst Turbo GreenMaster, 0.035 mM biotin-16-dUTP, 0.2 μ M F3/B3 outer primers, 1.6 μ M FIP/BIP inner primers, 0.4 μ M LF/LB loop primers and 100 ng template DNA (if not stated otherwise) in 10 μ L reaction volume. The LAMP reaction was conducted at 62 °C for 30 min without Bst polymerase inactivation. A sample without the template DNA was used as negative control. The LAMP reaction products were visualized by agarose electrophoresis using a 1.5% gel in 0.5 \times TBE buffer containing GelRed nucleic acid gel stain diluted 1:10 000 in water.

Magnetic Beads Preparation: Magnetic beads (MBs) were conjugated with amino-containing capture probes as follows: 20 μ L of magnetic beads were washed three times with 190 μ L of 25 mM MES buffer (pH 5.0) for 10 min at room temperature (RT) with rotation, followed by resuspension in 25 mM MES buffer. Then, 20 μ L of 100 μ M LNA or DNA capture probe (2 nmol) was added to the MBs and incubated for 30 min at RT without a washing step. Next, 30 μ L of 100 mg mL^{-1} EDC dissolved in MES buffer was added to the unwashed MB solution and incubated overnight at 4 °C. The CP-modified MBs were then washed thrice with 190 μ L of PBS, followed by the addition of 200 μ L of 0.02% sodium azide (in PBS), and stored at 4 °C for future use. All the incubation steps were performed using a rotator (20 rpm). The amount of modified MBs in the final suspension was determined by optical density measurements (Eppendorf 6131 Biophotometer Spectrometer). 5 μ L of the magnetic bead suspension was added to 1 mL of water in a cuvette, and the optical density of suspension at 600 nm (OD600) was read. This absorbance value was used to normalize the final MB volume for the hybridization reaction across all batches (Table S7, Supporting Information).

Hybridization on Magnetic Beads and EC Measurement: LNA- or DNA-conjugated MBs (volumes calculated from spectrophotometry measurements) were washed three times with WB and incubated in 25 μ L of hybridization solution (0.3 M NaCl containing 3.5 μ L of LAMP product) at 40 °C for 15 min. The modified MBs were then washed three times with CBB and incubated with SPP diluted 1:1000 in CBB at RT for 15 min. CBB was used to prevent non-specific binding of SPP to the MBs. Finally, the MBs were washed three times with PB, followed by resuspension of MBs with 10 μ L of PB. The final MB suspension (10 μ L) was transferred to a carbon working electrode with a magnetic support placed below. All three electrodes were covered with 50 μ L of PB solution containing 10 mM hydroquinone and 50 mM hydrogen peroxide as enzymatic substrates for SPP. Amperometry was performed at –0.3 V for 60 s to monitor the electric current from the enzymatic reaction.

Droplet Digital PCR (ddPCR): For the analysis, a commercial kit was used using specific and pre-validated probes provided by the manufacturer (Bio-Rad). The method was optimized using a cancer cell line (HT-29) containing the BRAF gene mutation to define the threshold set up needed for the correct absolute quantification of ddPCR results. The reaction conditions were applied to the samples. The final reaction mix contained 17 μ L of 1 \times ddPCR Supermix for Probes (no dUTP) and 1 \times Multiplex Primer FAM + HEX. The mixture was then pipetted onto a High-Profile 96-Well PCR plate, and 5 μ L of cfDNA was added to a final volume of 22 μ L per well. Subsequently, the plate was sealed using a PX1 PCR Plate Sealer and inserted into an Automated Droplet Generator system (Bio-Rad) to prepare the water-oil emulsion of the samples. PCR was performed in a C1000 Touch Thermal Cycler as follows: 1 cycle of enzyme activation at 95 °C for 10 min, 40 cycles of denaturation at 94 °C for 30 s, 1 cycle of annealing and extension at 55 °C for 1 min, 1 cycle of enzyme deactivation at 98 °C for 10 min, followed by an infinite hold at 4 °C. The plate was inserted into a QX200 Droplet Reader device to analyze all droplets using a two-color detection system. The results were plotted on a graph of fluorescence intensity using the QuantaSoft Software (Bio-Rad). The threshold distinguishing the positive and negative droplets was set up manually with respect to the positive and negative controls

(representative graph in Figure S9C, Supporting Information). HT-29 cell line was used as a positive control. Deionized water was used as the negative control.

Data Analysis: The Mann–Whitney test was used to determine whether there was a significant difference between the wild-type and mutated samples. Data for *p*-value calculations were obtained from the mean values of EC signals, that is, from at least two independent chronoamperometric measurements. The *p*-value below 0.05 was considered significant. The *BRAF*/*ACTB* ratio was calculated by dividing the EC current means for *BRAF* and *ACTB*. Sensitivity, specificity, positive predictive value, and negative predictive value were calculated using the chi-square test of independence. All analyses were performed using the GraphPad Prism software (version 7.03).

Experimental Ethics: The study received ethical approval from the Ethical Committee of the Masaryk Memorial Cancer Institute in Brno, and informed consent was obtained from all patients. All experiments were performed in compliance with relevant laws and institutional guidelines and in accordance with the ethical standards of the Declaration of Helsinki.

Supporting Information

Supporting Information is available from the Wiley Online Library or from the author.

Acknowledgements

L.M. and J.S. contributed equally to this work. The financial support of the Czech Health Research Council (No. NU21-08-00078 and NU21-09-00031), project SALVAGE (OP JAC; reg. no. CZ.02.01.01/00/22_008/0004644) – co-funded by the European Union and by the State Budget of the Czech Republic, BBMRI.cz (No. LM2023033) and MH CZ – DRO (MMCI, 00209805) is greatly acknowledged.

Conflict of Interest

The authors declare no conflict of interest.

Data Availability Statement

The data that support the findings of this study are available from the corresponding author upon reasonable request.

Keywords

cancer biomarker, circulating tumor DNA, electrochemical analysis, loop-mediated isothermal amplification, single-nucleotide polymorphism, V600E point mutation

Received: August 26, 2024

Revised: November 8, 2024

Published online:

- [1] a) P. A. Ascierto, J. M. Kirkwood, J.-J. Grob, E. Simeone, A. M. Grimaldi, M. Maio, G. Palmieri, A. Testori, F. M. Marincola, N. Mozzillo, *J. Transl. Med.* **2012**, *10*, 85; b) D. Bhamidipati, A. Pellatt, V. Subbiah, *JCO Precis Oncol* **2024**, *8*, 2300670.
- [2] L. Cheng, A. Lopez-Beltran, F. Massari, G. T. MacLennan, R. Montironi, *Mod Pathol* **2018**, *31*, 24.

- [3] a) D. Barras, *Biomark. Cancer* **2015**, *7*, 9; b) E. M. Polyanskaya, M. I. Fedyanin, *JMO* **2023**, *25*, 123.
- [4] C. Robert, B. Karaszewska, J. Schachter, P. Rutkowski, A. Mackiewicz, D. Stroiakovski, M. Lichinitser, R. Dummer, F. Grange, L. Mortier, V. Chiarion-Sileni, K. Drucis, I. Krajsova, A. Hauschild, P. Lorigan, P. Wolter, G. V. Long, K. Flaherty, P. Nathan, A. Ribas, A.-M. Martin, P. Sun, W. Crist, J. Legos, S. D. Rubin, S. M. Little, D. Schadendorf, *NEJM* **2014**, *372*, 30.
- [5] a) G. V. Long, J. S. Weber, J. R. Infante, K. B. Kim, A. Daud, R. Gonzalez, J. A. Sosman, O. Hamid, L. Schuchter, J. Cebon, R. F. Kefford, D. Lawrence, R. Kudchadkar, H. A. Burris3rd, G. S. Falchook, A. Algazi, K. Lewis, I. Puzanov, N. Ibrahim, P. Sun, E. Cunningham, A. S. Kline, H. Del Buono, D. O. McDowell, K. Patel, K. T. Flaherty, *J. Clin. Oncol.* **2016**, *34*, 871; b) G. V. Long, D. Stroyakovskiy, H. Gogas, E. Levchenko, F. de Braud, J. Larkin, C. Garbe, T. Jouary, A. Hauschild, J.-J. Grob, V. Chiarion-Sileni, C. Lebbe, M. Mandalà, M. Millward, A. Arance, I. Bondarenko, J. B. A. G. Haanen, J. Hansson, J. Utikal, V. Ferraresi, N. Kovalenko, P. Mohr, V. Probachai, D. Schadendorf, P. Nathan, C. Robert, A. Ribas, D. J. DeMarini, J. G. Irani, S. Swann, et al., *Lancet* **2015**, *386*, 444.
- [6] J. Tabernero, A. Grothey, E. Van Cutsem, R. Yaeger, H. Wasan, T. Yoshino, J. Desai, F. Ciardiello, F. Loupakakis, Y. S. Hong, N. Steeghs, T. K. Guren, H. T. Arkenau, P. Garcia-Alfonso, E. Elez, A. Gollerkeri, K. Maharry, J. Christy-Bittel, S. Kopetz, *J. Clin. Oncol.* **2021**, *39*, 273.
- [7] M. F. Sanmamed, S. Fernández-Landázuri, C. Rodríguez, R. Zárate, M. D. Lozano, L. Zubiri, J. L. Perez-Gracia, S. Martín-Algarra, A. González, *Clin. Chem.* **2015**, *61*, 297.
- [8] F. Spagnolo, P. Ghiorzo, L. Orgiano, L. Pastorino, V. Picasso, E. Tornari, V. Ottaviano, P. Queirolo, *Onco Targets Ther* **2015**, *8*, 157.
- [9] a) J. Braune, L. Keller, F. Schiller, E. Graf, D. Rafei-Shamsabadi, J. Wehrle, M. Follo, U. Philipp, S. Hussung, D. Pfeifer, M. Mix, J. Duyster, R. Fritsch, D. von Bubnoff, F. Meiss, N. von Bubnoff, *JCO Precis Oncol* **2020**, *4*, 20; b) M. Schreuer, G. Meersseman, S. Van Den Herrewegen, Y. Jansen, I. Chevolet, A. Bott, S. Wilgenhof, T. Seremet, B. Jacobs, R. Buyl, G. Maertens, B. Neyns, *J. Transl. Med.* **2016**, *14*, 95; c) L. F. Ye, Z. Y. Huang, X. X. Chen, Z. G. Chen, S. X. Wu, C. Ren, M. T. Hu, H. Bao, Y. Jin, F. Wang, F. H. Wang, Z. M. Du, X. Wu, H. Q. Ju, Y. Shao, Y. H. Li, R. H. Xu, D. S. Wang, *Drug Resist Updat* **2022**, *65*, 100883.
- [10] Y. Zhao, F. Chen, Q. Li, L. Wang, C. Fan, *Chem. Rev.* **2015**, *115*, 12491.
- [11] a) M. Anton, L. Moranova, R. Hrstka, M. Bartosik, *Anal. Methods* **2020**, *12*, 822; b) M. Bartosik, L. Jirakova, M. Anton, B. Vojtesek, R. Hrstka, *Anal. Chim. Acta* **2018**, *1042*, 37; c) N. Izadi, R. Sebuyoya, L. Moranova, R. Hrstka, M. Anton, M. Bartosik, *Anal. Chim. Acta* **2021**, *1187*, 339145; d) L. Moranova, M. Stanik, R. Hrstka, S. Campuzano, M. Bartosik, *Talanta* **2022**, *238*, 123064; e) R. Sebuyoya, L. Moranova, N. Izadi, L. Moran, R. Hrstka, M. Anton, M. Bartosik, *Biosens. Bioelectron* **2022**, *12*, 100224; f) L. Jirakova, R. Hrstka, S. Campuzano, J. M. Pingarron, M. Bartosik, *Electroanalysis* **2019**, *31*, 293; g) E. Povedano, V. R. V. Montiel, M. Gamella, V. Serafin, M. Pedrero, L. Moranova, M. Bartosik, J. J. Montoya, P. Yanez-Sedeno, S. Campuzano, J. M. Pingarron, *Anal. Bioanal. Chem.* **2020**, *412*, 5031; h) R. Sebuyoya, A. Valverde, L. Moranova, J. Strmiskova, R. Hrstka, V. R.-V. Montiel, J. M. Pingarron, R. Barderas, S. Campuzano, M. Bartosik, *Sens. Actuators B Chem* **2023**, *394*, 134375.
- [12] a) C. Zhang, Y. Yao, J.-L. Zhu, S.-N. Zhang, S.-S. Zhang, H. Wei, W.-L. Hui, Y.-L. Cui, *Sci. Rep.* **2016**, *6*, 26533; b) S. Yongkiettrakul, J. Kampeera, W. Chareanchim, R. Rattanajak, W. Pornthanakasem, W. Kiatpathomchai, D. Kongkasuriyachai, *Parasitol. Int* **2017**, *66*, 964; c) X. Liu, C. Zhang, M. Zhao, K. Liu, H. Li, N. Li, L. Gao, X. Yang, T. Ma, J. Zhu, W. Hui, K. Hua, Y. Cui, *Biosens. Bioelectron.* **2018**, *115*, 70.

- [13] T. Mana, B. Bhattacharya, H. Lahiri, R. Mukhopadhyay, *ACS Omega* **2022**, 7, 15296.
- [14] S. Fridland, J. Choi, M. Nam, S. J. Schellenberg, E. Kim, G. Lee, N. Yoon, Y. K. Chae, *J ImmunoTher Cancer* **2021**, 9, 002551.
- [15] S. Dey, K. M. Koo, Z. Wang, A. A. I. Sina, A. Wuethrich, M. Trau, *Lab Chip* **2019**, 19, 738.
- [16] G. Udayan, A. Marsella, P. Valentini, *Nanoscale* **2020**, 12, 2973.
- [17] L. Zhang, J. Peng, J. Chen, L. Xu, Y. Zhang, Y. Li, J. Zhao, L. Xiang, Y. Ge, W. Cheng, *Anal. Chem.* **2021**, 93, 5621.
- [18] Y. Liu, N. Lyu, V. K. Rajendran, J. Piper, A. Rodger, Y. Wang, *Anal. Chem.* **2020**, 92, 5708.
- [19] a) Y. Du, A. Pothukuchy, J. D. Gollihar, A. Nourani, B. Li, A. D. Ellington, *Angew Chem Int Ed* **2017**, 56, 992; b) M. Varona, D. R. Eitzmann, J. L. Anderson, *Anal. Chem.* **2021**, 93, 4149.
- [20] a) Y. S. Jiang, S. Bhadra, B. Li, Y. R. Wu, J. N. Milligan, A. D. Ellington, *Anal. Chem.* **2015**, 87, 3314; b) M. Varona, D. R. Eitzmann, D. Pagariya, R. K. Anand, J. L. Anderson, *Anal. Chem.* **2020**, 92, 3346.
- [21] G. Papadakis, A. K. Pantazis, N. Fikas, S. Chatzioannidou, V. Tsiakalou, K. Michaelidou, V. Pogka, M. Megariti, M. Vardaki, K. Giarentis, J. Heaney, E. Nastouli, T. Karamitros, A. Mentis, A. Zafiropoulos, G. Sourvinos, S. Agelaki, E. Gizeli, *Sci. Rep.* **2022**, 12, 3775.